Non-Pneumatic Wheel design performance for Human Powered Vehicles. Case: NASA HERC

Alvaro D. Callata Suxo, Fabio R. Diaz Palacios, Laura L. Choque Mamani
Marcelo A. Velasquez Enriquez, Mariel G. Valeriano Ramos, Adrián E. Vargas Llanquipacha
Adrian F. Acarapi Roca, Dayana R. Andrade Roque and Neil A. Campos Angulo
Universidad Catolica Boliviana, Mechatronic Engineer Department (CIDIMEC)
alvaro.callata, fdiaz, laura.choque, marcelo.enriquez, mariel.valeriano
adrian.acarapi, dayana.andrade and neil.campos@ucb.edu.bo

Abstract - This research addresses the design and manufacture of non-pneumatic tires (NPTs) using additive manufacturing (AM) for human-powered vehicles (HPVs) in challenging terrains, such as those present in competitions like NASA's Human Exploration Rover Challenge (NASA HERC). Traditional tires, prone to punctures and with high maintenance requirements, are less effective in these environments. In contrast, NPTs offer puncture resistance and low maintenance, but their design involves complex challenges in terms of load-carrying capacity, traction and durability. AM overcomes these challenges by enabling the creation of intricate geometries and internal structures optimized to match the terrain. In addition, the study focuses on flexible materials such as thermoplastic polyurethane (TPU), evaluating the impact of different AM processes on the mechanical properties and performance of TPNs. Through experimental and field-specific tests, we seek to optimize NPT designs, meeting high performance requirements and promoting sustainable manufacturing practices.

Index Terms—**3D printing, FDM technology, additive manufacturing, non-pneumatic wheels, modular design, terrain adaptability.**

I. Introduction

A. 3D Printing Technology

3D printing is an innovative technology that has already revolutionized many industries by allowing for the rapid fabrication of complex designs. It promotes innovation by making it possible to explore new design possibilities that were previously unattainable [1].

In the automotive sector, 3D printing is a promising method for producing lightweight components faster and more efficiently. This technology also encourages iterative design, facilitating continuous improvement through testing [2].

By taking advantage of materials such as TPU, which enables the creation of flexible and shock-absorbing components, manufacturers can modify the structural density to achieve the desired properties of each part depending on its specific function [3].

Modularity in 3D printing is essential for optimizing manufacturing and reducing costs. By allowing the creation of interchangeable components, modularity makes it easier to assemble and fit product parts efficiently. This approach also simplifies maintenance and repair by allowing replacement of specific parts without the need to rebuild the entire system. The ability to flexibly integrate modules contributes to greater efficiency in the manufacturing process and a significant reduction in associated costs [4].

3D printing contributes to sustainable manufacturing by minimizing material waste through an additive approach, which builds objects layer by layer from digital models. This process significantly reduces the amount of waste generated compared to traditional methods, which typically cut or mold materials into final shapes. Additionally, 3D printing allows the use of recyclable and eco-friendly materials, thus supporting more sustainable manufacturing practices [5].

B. Background - NASA HERC

Non-pneumatic wheels are a key solution to meet the challenges in competitions such as NASA HERC, where components capable of operating in extreme conditions are required. These wheels must offer traction and durability without the use of air, using innovative materials and structures that mimic the functions of traditional wheels but without the problems associated with air pressure.

In the NASA HERC competition, terrain analysis is crucial to the development of a rover capable of navigating simulated conditions on Mars and the Moon. The terrain features features such as cross-tilt slopes, rocks, gravel, regolith, cracks, and undulating irregular surfaces that pose significant challenges to the rover's mobility and stability. It offers us advantages for design and performance, giving us greater flexibility and sustainability.

1) Goal and Scopes (HERC)

The project aimed to cover a distance of half a mile in 8 minutes, overcoming various terrains simulating the lunar environment. Each challenge presented different obstacles where the wheels had to withstand loads, maintain traction, and facilitate the Rover vehicle's movement during the competition [6].

After analyzing possible solutions for a vehicle weighing approximately 70 kg, a custom wheel concept was developed to meet the following criteria:

- Improve vehicle grip: Wheels were designed with a V-pattern, optimizing the vehicle's traction with the ground surface and ensuring better performance on uneven terrains.
- Minimize weight: An optimal design was sought to make the wheels as light and strong as possible, reducing the vehicle's total weight and improving its efficiency.

- Modular design: A modular design was implemented for the wheels, allowing for quick and easy repairs in case of damage, ensuring better performance during the competition.

To achieve these objectives, advanced materials and innovative manufacturing techniques were used. The wheels were made with flexible and durable plastics, specifically elastomers, offering high resistance to abrasion, cracking, and dynamic loads. The tires were produced using the fused deposition modeling (FDM) method, allowing for adjustable infill density and stiffness modification according to the design needs. [7]

II. Design

A. Iterative Design - Wheel Tread

As previously mentioned, the proposed design is intended for the NASA HERC. Throughout the construction process, the design underwent significant changes, resulting in improvements in size, weight, and overall design.

Fig. 1: Wheel design focused on pressure points.

The presented design in Figure 1 is based on a pressure point approach, where it was crucial for the tire's tread to be narrow and follow a traditional tread pattern similar to that of off-road tires. The primary goal of this model was to create a robust, wide, and durable traction system capable of withstanding a variety of challenging terrains. However, while the initial design met these objectives, it also posed significant challenges. The system's excessive size, combined with the substantial amount of materials required for its construction, resulted in an inefficient model. This led to a revision and redesign, focusing on a more efficient and optimized traction system. The new design aimed to maintain the ability to tackle rough terrains but with a lighter, more compact structure that required fewer resources in terms of materials and assembly. This approach not only reduced the system's weight and size but also enhanced its overall performance, improving its adaptability to the demands of the competition. The new design was inspired by mountain bike wheels (Figure 2), incorporating key features that enhance both strength and adaptability to challenging terrains. At the heart of the design is a robust structure made of 1060 aluminum, chosen for its excellent balance of lightness and durability. This central structure is surrounded by aluminum circumferences that act as shock absorbers, designed with internal veins to prevent deformation under heavy loads and impacts. The tread design was based on two distinct mountain bike models, each optimized for different terrain conditions:

Fig. 2: Mountain Wheel-Based Model

- V-Shaped Design: This pattern was created to maximize traction by providing a surface that effectively grips the terrain. Additionally, the design allows water to be channeled to the sides, improving performance in wet or rainy conditions by preventing hydroplaning.
- Lightning Design: This model is characterized by offering greater friction with the ground, providing exceptional grip, especially on flat terrain. While this design increases resistance during rolling, it benefits from enhanced stability on smooth surfaces, ensuring that the vehicle maintains a steady and controlled path.

These two design options allow the vehicle to adapt to a variety of conditions, combining traction, durability, and responsiveness depending on the terrain and the specific needs of the competition.

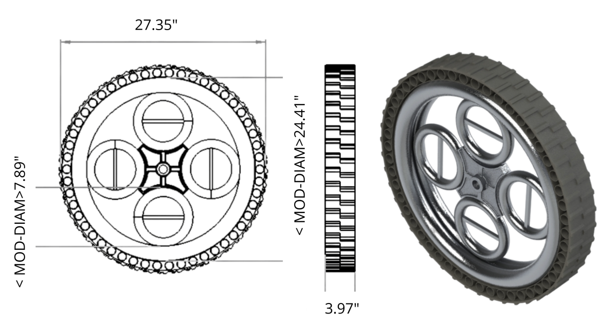

Fig. 3: Robust 4-ring model

Finally, a hybrid design was chosen that provides effective adaptation to various terrains (Figure 3). This design strikes a balance with an adequate width to ensure stability without being overly bulky. Its lightweight construction allows for good impact absorption. The tread pattern is designed to grip the terrain effectively, minimizing movement during travel and ensuring consistent traction throughout the competition. Once the design was finalized, it was modeled to meet the following parameters: the wheel is constructed from 1060 aluminum with a tubular structure, featuring a diameter of 25.5 inches and a width of 4 inches. The tread design is intended to cover the entire surface, achieving symmetry that helps absorb shocks from the terrain. The arrangement of the aluminum tubes contributes to increased traction, optimizing the vehicle's performance.

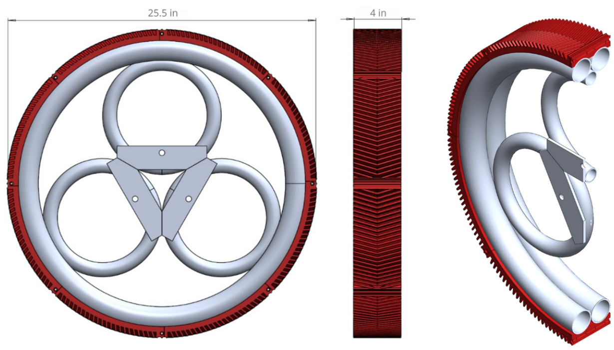

Fig. 4: Final Wheel Mode with 3-ring

This approach ensures that the wheel is not only durable and capable of withstanding various impacts but also provides reliable performance across different types of terrain, maintaining stability and traction throughout the competition. To ensure that the non-pneumatic wheels, as shown in Figure 4, meet the performance requirements for the NASA HERC event, detailed simulations were conducted to model their behavior under various load and terrain conditions.

B. Stress Analysis

To perform an adequate stress analysis on the wheel, it is essential to consider the following technical specifications (Table I):

TABLE I: Wheel Specifications

Description	**Value**
Wheel diameter	25.5 [in]
Contact area width	4 [in]
Wheel weight	12 [kg]
Number of wheels	4

In this analysis, the stress on an aluminum wheel of a vehicle with a mass of 70 kg (total mass including drivers: 200 kg) is evaluated. The vehicle has four wheels, and the load is assumed to be evenly distributed among them. We will calculate the contact pressure, Von Mises stress, and the safety factor for the aluminum wheel material based on these assumptions.

Load Calculation per Wheel

The total load on the vehicle, including the drivers, is 200 kg. This mass results in a gravitational force F_g acting on the system, calculated as:

$$F_g = m_{total} \cdot g = 200\,\text{kg} \cdot 9.81\,\text{m/s}^2 = 1962\,\text{N} \tag{1}$$

Since the vehicle has four wheels, the load per wheel is determined by:

$$F_{wheel} = \frac{F_g}{n_{wheels}} = \frac{1962\,\text{N}}{4} = 490.5\,\text{N} \tag{2}$$

This evenly distributed force simplifies the stress analysis by considering a uniform load on each wheel.

Pressure Calculation over the Contact Area

The pressure exerted on the wheel is calculated based on the contact area between the wheel and the ground. The wheel has a diameter of 0.648 m and a contact width of 0.1 m. Therefore, the contact area is given by:

$$A = d_{wheel} \cdot A_{contact} = 0.648\,\text{m} \cdot 0.1\,\text{m} = 0.0648\,\text{m}^2 \tag{3}$$

The pressure P acting on the contact area is then:

$$P = \frac{F_{wheel}}{A} = \frac{490.5\,\text{N}}{0.0648\,\text{m}^2} = 7567.59\,\text{Pa} \tag{4}$$

This pressure provides a measure of the normal stress acting on the surface of the wheel due to the load.

Von Mises Stress Calculation

For ductile materials such as aluminum, the von Mises stress criterion is used to predict yielding under a complex state of stress. The von Mises stress σ_v is calculated using the principal stresses σ_1 and σ_2. The equation is:

$$\sigma_v = \sqrt{\sigma_1^2 - \sigma_1\sigma_2 + \sigma_2^2} \tag{5}$$

In this case, the principal stress σ_1 is equal to the pressure P, and since we assume no lateral stresses, σ_2 is zero:

$$\sigma_1 = P = 7567.59\,\text{Pa}, \quad \sigma_2 = 0\,\text{Pa} \tag{6}$$

Substituting these values into the von Mises equation:

$$\sigma_v = \sqrt{7567.59^2 + 0^2 - 7567.59 \cdot 0} = 7567.59\,\text{Pa} \tag{7}$$

This value represents the equivalent stress that would cause yielding in the material under the given loading conditions.

Safety Factor Calculation

The safety factor is calculated to determine the margin of safety of the design. For aluminum, the yield strength is typically $\sigma_{yield} = 275\,\text{MPa}$. The safety factor FS is defined as the ratio of the yield strength to the applied von Mises stress:

$$FS = \frac{\sigma_{yield}}{\sigma_v} = \frac{275 \times 10^6\,\text{Pa}}{7567.59\,\text{Pa}} = 36.34 \tag{8}$$

This high safety factor indicates that the wheel design is well within the acceptable limits, suggesting a robust design against the applied stresses.

Von Mises Stress Simulation

Stress simulations are useful for validating the mechanical strength and durability of components under operational loads. This section presents the von Mises stress analysis of two key components of the rover: the aluminum wheel ring and the TPU tread designs. These analyses aim to identify potential failure points and ensure the designs meet performance and safety requirements under expected and extreme conditions.

1) Aluminum Ring Simulation

The aluminum ring are the structural element of the rover's wheel, ensuring that it remains stable during rotation and load-bearing activities. Aluminum was chosen for its balance between strength and lightness, essential for maintaining the rover's mobility. This analysis evaluates the ring's behavior under applied stresses to confirm that it can safely withstand dynamic forces encountered during operation.

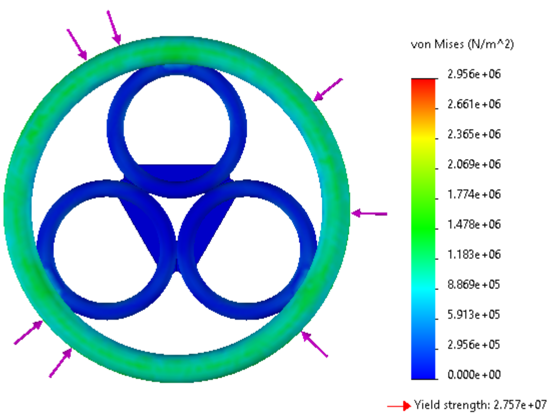

Fig. 5: Von Mises analysis of the wheel's aluminum ring.

The von Mises stress simulation for the aluminum ring used a uniformly applied force of 500[kg] across the wheel's surface. The goal was to assess the ring's capacity to endure high operational loads and identify any stress concentrations that might pose a risk during rotation. The results confirm that the design is structurally sound under these conditions, ensuring reliable performance even under heavy loads.

2) Tread Simulation

The TPU tread provides traction and shock absorption on uneven terrains. TPU is favored for its flexibility and toughness, but understanding how stress distributes across the tread structure is essential to optimize performance and prevent premature wear. The following analyses focus on two different tread designs to evaluate their strength, durability, and suitability for varied terrain conditions.

The first tread design was tested with a total load of 500 [kg] distributed across four wheels. The analysis shows the tread maintains structural integrity at stress levels up to 2.5×10^5 N/m^2. The analysis highlighted areas of concern in the lower regions of the "spikes," where stress levels reached 4.5×10^5 [N/m^2], indicating potential vulnerability.

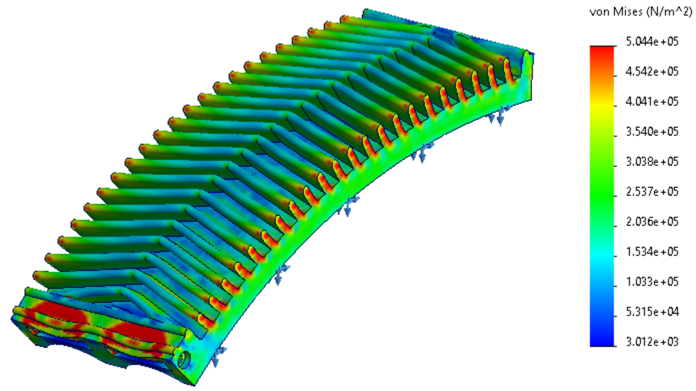

Fig. 6: Von Mises analysis of the first tread design.

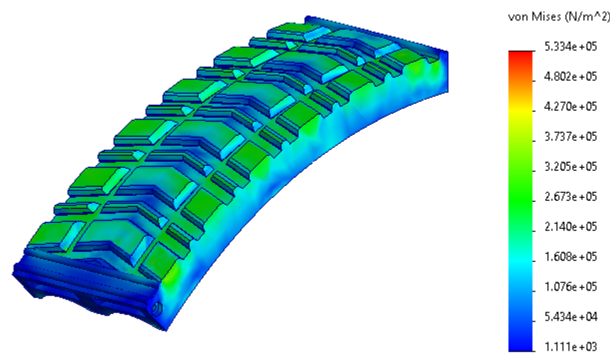

Fig. 7: Von Mises analysis of the second tread design.

The second tread design, featuring a honeycomb pattern for improved cushioning, was analyzed under a load of 500[kg]. The results indicate that the design can withstand the applied forces but suggest keeping stress below 3.8×10^5 N/m^2 to ensure durability. While the honeycomb structure improves shock absorption and provides better weight distribution, it reduces grip and limits surface contact with the ground, potentially affecting performance on challenging terrains.

C. 3D Printing Process

Two distinct wheel tread designs were developed, each carefully considering the specific traction and cushioning requirements of the vehicle as shown in Figures 5 and 6

In the upper panel of figure 9 and figure 8, it can be observed the tread aimed to provide traction to the vehicle, having a design that provides more stiffness and provides traction due to its geometry. In the lower panel of figure 9 and figure 8, the tread designed to provide cushioning to the vehicle can be observed, taking advantage of the infill that will be applied during 3D printing, so it will have a cushioning effect on the performance of the vehicle.

Both pieces should be printed in a flexible material such as TPU to properly provide the characteristics expected of each footprint design. Factors such as relatively low layer adhesion when working with TPU, delamination, use of support structures, infill density and tensile strength are parameters that

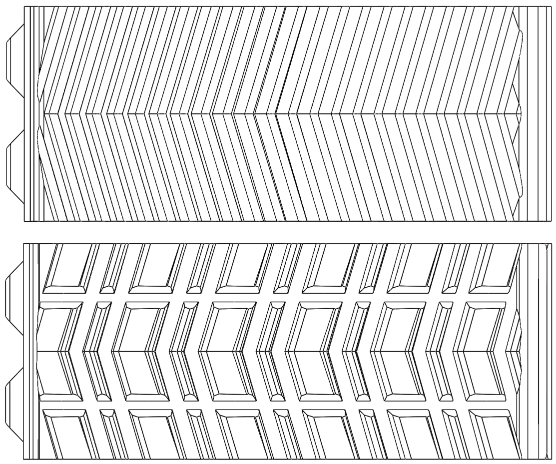

Fig. 8: Top view of the first tread design (top); and second tread design (bottom).

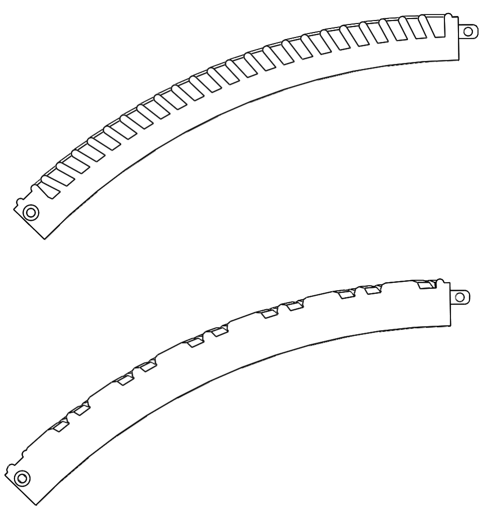

Fig. 9: Side view of the first tread design (top); and second tread design (bottom).

must be taken into account when planning to 3D print parts with TPU.

By decreasing the printing speed, increasing the printing temperature, and raising the infill density, improvements in layer adhesion as well as tensile strength are demonstrated [8].

FDM technology was successfully applied to 3D print non-pneumatic tires based on TPU material, showing that the three-dimensional stiffness obtained is basically 50% of that obtained by simulation [9].

The isometric view 10 also considers the shape and diagonal position relative to the base on which it was printed. The layers were adhered in the same direction as the traction generated when making contact with the surface, which makes it more resistant to tensile and bending stresses. Additionally, this approach helps prevent filament separation in the layer adhesion.

The cross-sectional view of the model is observed in Figure

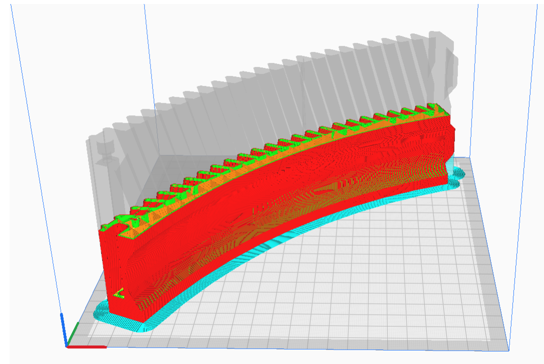

Fig. 10: Model isometric view

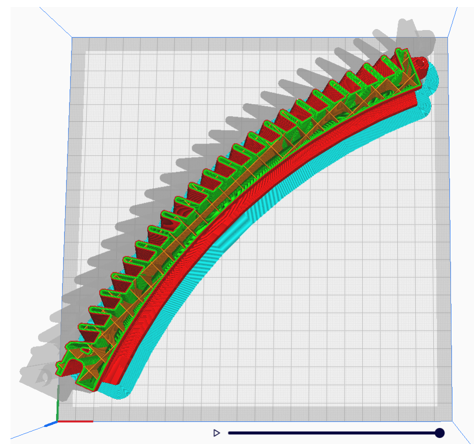

Fig. 11: Model section view

11, which shows a square-shaped infill structure. This allowed for a cushioning reaction during its application on the track.

III. Results

A. Analysis Results

The analysis carried out on the vehicle wheels reveals that the vertical load supported by each wheel is 171.5 N, distributing the total weight equally between the four wheels. In addition, the lateral force experienced during a turn is 30.625 N, which is relevant to assess the stability of the vehicle under dynamic conditions. The normal stress, determined as 1715.0 N/m, together with the Von Mises stress calculated at 3364.9 N/m, allow the structural behaviour of the wheels to be predicted under different loads. When comparing these values with tyres commonly used in cars, it can be seen that the analysed wheels have a considerably lower load capacity, a smaller contact area, and support significantly lower stresses. Since they are designed for light vehicles, as opposed to commercial tires that must withstand greater forces and stresses under everyday use conditions, they are very easy to obtain since they are based on 3D printing that can be done in outer space, in addition to their low cost and easy production, proving to be resistant for light space vehicles.

The results showed that the outer rim, in direct contact with the ground, experienced minimal deformation of 3.548 N/m^2. This deformation is insignificant and does not affect the wheel's functionality. The inner rings, responsible for structural support, showed no significant deformation, confirming that they provide adequate reinforcement. These results validate the wheel's capacity to withstand high loads while maintaining structural integrity.

To ensure structural integrity and optimize performance, we conducted a Von Mises stress analysis on the TPU rover treads. Our analysis revealed that while both initial and honeycomb-infill designs could effectively support the applied force of 137200[N] distributed across four wheels, stress concentrations were observed in specific areas. For the initial design, exceeding a stress level of 2.2×10^5 [N/m^2], particularly in the lower regions of the "spikes" where stress reached 3.54×10^5 [N/m^2], is not recommended. Similarly, for the honeycomb-infill design, maintaining stress levels below 1.28×10^5 [N/m^2] is advisable to prevent potential failure, despite the enhanced cushioning effect this structure provides.

TABLE II: Results of the forces and stresses calculations on the wheels

Parameter	Value
Vertical load per wheel (F_{wheel})	171.5 N
Lateral force (F_{lat})	30.625 N
Normal stress (σ)	1715.0 N/m
Von Mises stress (σ_{vm})	3364.86 N/m
Contact area	0.10 m
Lateral acceleration (a_{lat})	1.75 m/s²
Number of wheels	4

B. Manufacturing

1) Mechanical process

The fabrication of the four complete aluminum rings, crafted from 6061 aluminum, involved utilizing tubes of varying dimensions. Following a preprocessing stage that included spiral bending, the rings were successfully formed to their desired shape. Each ring then underwent a thermal deformation process to seamlessly join its ends before being straightened.

Each complete ring comprises two larger tubes and three smaller tubes. The two larger tubes were meticulously assembled to create a single, robust double ring. Within this double ring, the three smaller rings were strategically arranged in a triangular configuration. To further enhance structural integrity, triangular plates were cut and assembled, then securely joined using TIG welding, as depicted in the Figure 4.

The total weight of each ring is approximately 8.82 lbs ± 0.22 lbs. With the addition of a plastic mount for the tire tread, the total weight increased to 13.23 lbs ± 0.44 lbs.

The dimensions, such as weight, diameter, weld width, and balance, were carefully verified to ensure uniformity and quality in each component.

2) 3D printing parameters

After testing and prototyping during the development of the parts, the data and settings relevant to 3D printing are collected in the table III, optimizing the manufacturing of the 3D printed parts used in the project and their intended purpose. These parameters have been carefully selected to ensure accuracy, strength and quality of the final parts.

TABLE III: Optimization of Parameters for 3D Printing

Parameter	Optimized value
Layer height	0.28 [mm]
First Layer height	0.2 [mm]
Wall thickness	1.2 [mm]
Number of perimeters	3
Printing speed	40 [mm/s]
Flow	100%
Extrusion temperature	225 °C
Build Plate temperature	40 °C
Build Plate adhesion	Brim
Retraction speed	45 [mm/s]
Retraction distance	5 [mm]
Number of solid layers	4

IV. Conclusions and Recommendations

The findings of this research highlight several key points related to the use of 3D printing in the design of non-pneumatic wheels for human-powered vehicles. The versatility of modularity in 3D printing plays a crucial role in the success of this design. By enabling interchangeable and easily replaceable components, the modular approach facilitates quick repairs and adjustments during demanding competitions, improving the adaptability and maintainability of the vehicle. This modularity not only optimizes manufacturing processes, but also reduces costs, as specific parts can be replaced without the need to recreate the entire system. This modularity is a clear advantage of 3D printing wheels applications, making it an ideal manufacturing approach for dynamic and rapidly changing conditions.

Another significant point is the fitting design derived from the intricate possibilities offered by 3D printing. The complexity of the design allows wheels to be precisely tailored to the performance demands of the terrain. For instance, V-band pattern designs were optimized to improve grip and stability, increasing the overall efficiency of the vehicle. The ability to adjust parameters such as infill density and structure through additive manufacturing makes it possible to achieve both strength and flexibility, essential for racing in extreme conditions. Taking advantage of the complexity in 3D design offers the ability to fine-tune performance with a high degree of precision.

Finally, the use of different materials, particularly those that are lightweight but durable, such as TPU, offers substantial advantages in weight optimization. Taking advantage of different materials allows for weight reduction without compromising performance, as these materials are flexible and resistant to mechanical stress. This weight optimization is crucial to improving vehicle efficiency, as a lighter vehicle requires less energy while maintaining its structural integrity. The combination of advanced materials and design complexity enables the creation of a highly efficient, durable, and sustainable wheel system for human-powered vehicles.

References

[1] S. F. Iftekar, A. Aabid, A. Amir, and M. Baig, "Advancements and Limitations in 3D Printing Materials and Technologies: A Critical Review," vol. 15, no. 11, p. 2519. [Online]. Available: https://www.ncbi.nlm.nih.gov/pmc/articles/PMC10255598/

[2] Y. Vashi, R. Anand, K. Jayakrishna, G. Rajyalakshmi, and S. A. Raj, “Design and analysis of 3D printed UAV wheel,” vol. 46, pp. 8307–8312. [Online]. Available: https://linkinghub.elsevier.com/retrieve/pii/S2214785321023488

[3] L. Rodríguez-Parada, S. d. l. family, and P. F. Mayuet, “Influence of 3D-Printed TPU Properties for the Design of Elastic Products,” vol. 13, no. 15, p. 2519. [Online]. Available: https://www.mdpi.com/2073-4360/13/15/2519

[4] P. M. Davies, “An investigation into modularity-in-context and 3d printing for resource integration: An operations management perspective.”

[5] S. P. Tadi, S. S. Maddula, and R. S. Mamilla, “Sustainability aspects of composite filament fabrication for 3d printing applications,” vol. 189, p. 113961. [Online]. Available: https://www.sciencedirect.com/science/article/pii/S1364032123008195

[6] NASA, *2023 Human Exploration Rover Challenge Handbook*, National Aeronautics and Space Administration, Washington, DC, USA, August 2023, last accessed: August 10, 2024. [Online]. Available: https://www.nasa.gov/wp-content/uploads/2023/08/herc-2023-handbook-final-edit-508.pdf

[7] A. ZAKRECKI, B. GACZOREK, K. BERENT, and A. KANIA, “projekt i wykonanie w technologii przyrostowej kół łazika marsjańskiego z wypełnienie strukturalnym” (project of mars rover wheels based on structural infill using additive manufacturing.” [Online]. Available: https://www.mechanik.media.pl/pliki/do$_{p}obrania/artykuly/22/2018_{0}3_{s}0244_{e}ng.pdf$

[8] S. M. Desai, R. Y. Sonawane, and A. P. More, “Thermoplastic polyurethane for three-dimensional printing applications: A review,” vol. 34, no. 7, pp. 2061–2082, _eprint: https://onlinelibrary.wiley.com/doi/pdf/10.1002/pat.6041. [Online]. Available: https://onlinelibrary.wiley.com/doi/abs/10.1002/pat.6041

[9] L. Rodríguez, G. Naya, and R. Bienvenido, “Study for the selection of 3d printing parameters for the design of TPU products,” vol. 1193, no. 1, p. 012035. [Online]. Available: https://iopscience.iop.org/article/10.1088/1757-899X/1193/1/012035